


# Computing Voronoi Diagrams in the Polar-Coordinate Model of the Hyperbolic Plane

Tobias Friedrich  

Hasso Plattner Institute, University of Potsdam  
Potsdam, Germany

Maximilian Katzmann  

Hasso Plattner Institute, University of Potsdam  
Potsdam, Germany

Leon Schiller  

Hasso Plattner Institute, University of Potsdam  
Potsdam, Germany

---

## Abstract

A Voronoi diagram is a basic geometric structure that partitions the space into regions associated with a given set of sites, such that all points in a region are closer to the corresponding site than to all other sites. While being thoroughly studied in Euclidean space, they are also of interest in hyperbolic space. In fact, there are several algorithms for computing hyperbolic Voronoi diagrams that work with the various models used to describe hyperbolic geometry. However, the *polar-coordinate model* has not been considered before, despite its increased popularity in the network science community. While Voronoi diagrams have the potential to advance this field, the model is geometrically not as approachable as other models, which impedes the development of geometric algorithms.

In this paper, we present an algorithm for computing Voronoi diagrams natively in the polar-coordinate model of the hyperbolic plane. The approach is based on Fortune’s sweep line algorithm for Euclidean Voronoi diagrams. We characterize the hyperbolic counterparts of the concepts it utilizes, introduce adaptations necessary to account for the differences, and prove that the resulting algorithm correctly computes the Voronoi diagram in time  $\mathcal{O}(n \log(n))$ .

**2012 ACM Subject Classification** Theory of computation  $\rightarrow$  Computational geometry; Theory of computation  $\rightarrow$  Data structures design and analysis

**Keywords and phrases** Voronoi diagram, hyperbolic geometry, polar coordinates, sweep line algorithm

## 1 Introduction

The Voronoi diagram is a fundamental and well-studied geometric structure. Given a set of points, which we call *sites*, the goal is to partition the space into *cells*, i.e., regions that are associated with the sites, such that no site is closer to a point in a cell than the associated one. Typically, the sites are assumed to lie in Euclidean space, where finding the Voronoi diagram or its geometric dual, the Delaunay triangulation, has various applications in biology, computer graphics, and robotics [5, 11, 14]. However, this problem is also relevant in hyperbolic geometry, in the context of finding certain Möbius transformations [2], computing Delaunay triangulations of points in two planes [8], or for greedy routing in networks [27].

Hyperbolic and Euclidean geometry differ in several fundamental properties. First, space expands exponentially fast in hyperbolic space, while the expansion is only polynomial in Euclidean space. Second, for a hyperbolic line there are infinitely many lines that go through a point not on the line and are parallel to the first one. And, third, in contrast to the flat Euclidean space, hyperbolic space is negatively curved.

Over time, various models have been developed to capture these properties and facilitate the study of hyperbolic geometry. While some models, like the *Poincaré ball*, the *Klein ball*, and the *hemisphere model* represent the infinite hyperbolic space in a finite region in

Euclidean space, other models like the *upper-half-plane model* and the *hyperboloid model* map it onto unbounded Euclidean regions. For an overview we refer the reader to [25, Chapter 7].

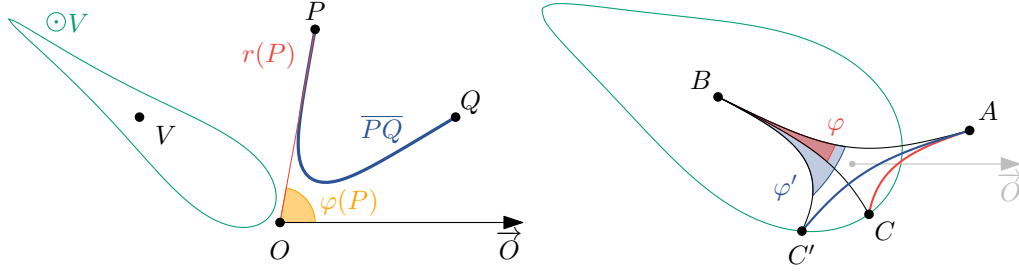
With the different models came different approaches to computing Voronoi diagrams. For the upper-half-plane model there is an algorithm that computes the hyperbolic Voronoi diagram from a Euclidean one [24]. A similar approach was later used to generalize an  $\mathcal{O}(n^2)$ -algorithm in the two-dimensional Poincaré disk [23], to an  $\mathcal{O}(n \log(n))$ -algorithm that works in the Poincaré ball of arbitrary dimensionality [6]. Another method is based on power diagrams and utilizes the Klein disk model [21]. We refer the reader to [27] for an overview of hyperbolic Voronoi diagrams, to [20] for their relation to hyperbolic delaunay triangulations, and to [22] for visualizations in different models. We note that converting between the various representations typically involves scaling the coordinates exponentially, which can lead to numerical issues. Consequently, it is best to perform all computations directly in one model, instead of taking detours through other representations.

A model that has not been considered in the context of hyperbolic Voronoi diagrams before is the *polar-coordinate model*, which is rather surprising given its growing popularity in the study of complex networks. There, the polar-coordinate representation is used to analyze real-world networks like protein-interaction networks, the internet, and trade networks [1, 7, 13]. In particular, *hyperbolic random graphs*, a generative graph model aimed at representing such networks, were introduced using the polar-coordinate model of the hyperbolic plane [16], and it was since shown that this representation is particularly well-suited for mathematical analysis of network properties and algorithms [3, 4, 15, 17, 19]. We believe that being able to compute Voronoi diagrams in this model has the potential to further advance this field.

One reason for the mathematical accessibility of the polar-coordinate model is its straightforward definition. Points in hyperbolic space are addressed using their distance to a dedicated point, called *pole*, and the angular distance to a ray starting at the pole, called *polar axis*. The resulting coordinates are then simply interpreted as polar coordinates in Euclidean space. However, in contrast to models like the Poincaré disk, where hyperbolic circles are Euclidean circles (with offset centers) and hyperbolic lines are circular arcs in Euclidean space, or the hyperboloid model, where hyperbolic circles and lines are intersections of planes with the hyperboloid, the polar-coordinate model is not as approachable from a geometric point of view. There, hyperbolic circles are shaped like tear drops and lines are hyperbolas that are bent towards the pole (see Figure 1 (left) for an illustration). As a consequence, this model has not been considered in the context of geometric algorithms before.

In this paper, we present an algorithm for computing Voronoi diagrams directly in the polar-coordinate model of the two-dimensional hyperbolic plane. The approach is based on Fortune’s sweep line algorithm for computing Voronoi diagrams in the Euclidean plane [12], which scans the plane and maintains data structures to incrementally build the diagram using a so-called *beach line*. More precisely, our approach builds on a generalization of Fortune’s algorithm that uses an expanding sweep circle instead of a line [28]. We characterize the structure and behavior of the beach-line equivalent in our hyperbolic sweep circle approach and prove that the corresponding algorithm correctly computes the hyperbolic Voronoi diagram in time  $\mathcal{O}(n \log(n))$ . This is optimal since, analogous to the Euclidean version [26, Theorem 6.14], computing the hyperbolic Voronoi diagram can be reduced to sorting.

The paper is structured as follows. We give an overview of our notation, an introduction to the polar-coordinate model, and a brief summary of Fortune’s algorithm and its generalization (Section 2). Afterwards, we describe the hyperbolic sweep circle approach (Section 3) and prove its correctness and running time complexity (Section 4). We conclude with an outlook on how the approach can be extended and utilized in the context of network science (Section 5).



■ **Figure 1 (Left)** The polar-coordinate model of the hyperbolic plane. Point  $P$  has distance  $r(P)$  to the pole  $O$  and angular distance  $\varphi(P)$  to the polar axis  $\vec{O}$ . The line segment  $\overline{PQ}$  is shown in blue. Point  $V$  is the center of the tear-drop shaped green circle  $\odot V$ . **(Right)** Illustration of the triangles  $\triangle ABC$  and  $\triangle ABC'$  from Lemma 1. Since  $C$  and  $C'$  lie on a circle (green) with center  $B$ , we have  $|\overline{BC}| = |\overline{BC'}|$ . When increasing the angle  $\varphi$  at  $B$  to  $\varphi'$  then  $|\overline{AC}| < |\overline{AC'}|$ .

## 2 Preliminaries

We denote points with capital letters like  $P, Q$  and sets or tuples with calligraphic capital letters like  $\mathcal{S}, \mathcal{V}$ . Given two points  $P, Q$ , we denote the line through them with  $\overleftrightarrow{PQ}$  and the ray from  $P$  through  $Q$  with  $\overrightarrow{PQ}$ . A ray starting at  $P$ , whose direction is given by context is denoted by  $\vec{P}$ . The line segment between  $P$  and  $Q$  is written as  $\overline{PQ}$  and  $|\overline{PQ}|$  denotes its length, i.e., the distance between  $P$  and  $Q$ . The *perpendicular bisector*, i.e., the set of points with equal distance to  $P$  and  $Q$  is denoted by  $P \perp Q$ . A *circle* with center  $P$ , i.e., the set of all points  $Q$  with equal distance to  $P$  is denoted by  $\odot P$ . The points  $Q$  are said to lie on the *arc* of  $\odot P$ . Triangles are written as  $\triangle PQS$  and  $\sphericalangle PQS$  denotes the angle between  $\overrightarrow{QP}$  and  $\overrightarrow{QS}$  measured in *clockwise* direction around  $Q$ . The intersection of two objects is denoted with a  $\cap$ -sign, e.g., the intersection of two line segments  $\overline{PQ}$  and  $\overline{ST}$  is denoted by  $\overline{PQ} \cap \overline{ST}$ .

**The Hyperbolic Plane.** In this paper, we work with the *polar-coordinate model* of the hyperbolic plane  $\mathbb{H}^2$ . There, points are identified using polar coordinates. After defining a designated *origin* or *pole*  $O \in \mathbb{H}^2$  together with a *polar axis*  $\vec{O}$ , i.e., a reference ray starting at  $O$ , a point  $P \in \mathbb{H}^2$  is identified using its *radius*  $r(P)$  denoting the hyperbolic distance to  $O$  and its *angle*  $\varphi(P)$  denoting the angular distance to  $\vec{O}$  in counterclockwise direction around  $O$ . For visualizations, these coordinates are then interpreted as polar coordinates in the Euclidean plane, as shown in Figure 1 (left). We note that angles at line intersections are *not* preserved by the projection and are only added in our figures for illustration purposes.

In contrast to Euclidean geometry, the sum of the inner angles of a triangle  $\triangle ABC$  does not equal  $\pi$  but is strictly less than  $\pi$  in the hyperbolic plane. Still, we can relate the length of the segment  $\overline{AB}$  to the lengths of the other two segments and the angle  $\varphi$  at  $C$ , using the *hyperbolic law of cosines*, which is defined as

$$\cosh(|\overline{AB}|) = \cosh(|\overline{AC}|) \cosh(|\overline{BC}|) - \sinh(|\overline{AC}|) \sinh(|\overline{BC}|) \cos(\varphi), \quad (1)$$

where  $\sinh(x) = (e^x - e^{-x})/2$ ,  $\cosh(x) = (e^x + e^{-x})/2$ . Analogous to Euclidean geometry, the hyperbolic tangent  $\tanh$  is defined as the quotient of the hyperbolic sine and cosine functions. We denote the inverse of the hyperbolic trigonometric functions with  $\operatorname{asinh}$ ,  $\operatorname{acosh}$ , and  $\operatorname{atanh}$ . Using the hyperbolic law of cosines we can derive that the hyperbolic distance between two points  $A, B \in \mathbb{H}^2$  is given by

$$|\overline{AB}| = \operatorname{acosh} \left( \cosh(r(A)) \cosh(r(B)) - \sinh(r(A)) \sinh(r(B)) \cos(\Delta_\varphi(A, B)) \right),$$

where  $\Delta_\varphi(A, B) = \pi - |\pi - |\varphi(A) - \varphi(B)||$  denotes the angular distance between  $A$  and  $B$ . We note, however, that since  $\cos(\pi - x) = -\cos(x)$  and since  $\cos(-x) = \cos(x)$ , the cosine of the angular distance is simply given by  $\cos(\Delta_\varphi(A, B)) = \cos(\varphi(A) - \varphi(B))$ . Thus, the above equation can be simplified to

$$|\overline{AB}| = \operatorname{acosh}(\cosh(r(A)) \cosh(r(B)) - \sinh(r(A)) \sinh(r(B)) \cos(\varphi(A) - \varphi(B))). \quad (2)$$

The hyperbolic distance between a circle  $\odot O$  of radius  $r$  centered at the pole and a point  $A$  with radius  $r(A) \leq r$  is given by  $r - r(A)$ . The following lemma shows that increasing (resp. decreasing) an angle in a triangle also increases (resp. decreases) the length of the opposite line segment, as illustrated in Figure 1 (right).

► **Lemma 1.** *Let  $\triangle ABC$  and  $\triangle ABC'$  be triangles with  $|\overline{BC}| = |\overline{BC'}|$  and angles  $\varphi$  and  $\varphi'$  at  $B$ , respectively. Then,  $\varphi < \varphi'$  (resp.  $\varphi > \varphi'$ ) if and only if  $|\overline{AC}| < |\overline{AC'}|$  (resp.  $|\overline{AC}| > |\overline{AC'}|$ ).*

**Proof.** We prove the claim for the case where  $\varphi < \varphi'$ . The proof for the other case is analogous. We start by showing that changing the angle also changes the length of the line segment accordingly. Since  $\varphi, \varphi'$  are inner angles of triangles, we have  $\varphi, \varphi' \in [0, \pi)$  and thus  $\cos(\varphi) > \cos(\varphi')$ . We can now determine  $|\overline{AC}|$  using the hyperbolic law of cosines and make use of the fact that  $|\overline{BC}| = |\overline{BC'}|$ , which yields

$$\begin{aligned} |\overline{AC}| &= \operatorname{acosh}(\cosh(|\overline{AB}|) \cosh(|\overline{BC}|) - \sinh(|\overline{AB}|) \sinh(|\overline{BC}|) \cos(\varphi)) \\ &= \operatorname{acosh}(\cosh(|\overline{AB}|) \cosh(|\overline{BC'}|) - \sinh(|\overline{AB}|) \sinh(|\overline{BC'}|) \cos(\varphi)) \\ &< \operatorname{acosh}(\cosh(|\overline{AB}|) \cosh(|\overline{BC'}|) - \sinh(|\overline{AB}|) \sinh(|\overline{BC'}|) \cos(\varphi')) \\ &= |\overline{AC'}|, \end{aligned}$$

where the inequality is due to the fact that  $\cos(\varphi) > \cos(\varphi')$  and that  $\operatorname{acosh}(x)$  is strictly increasing with increasing  $x$ .

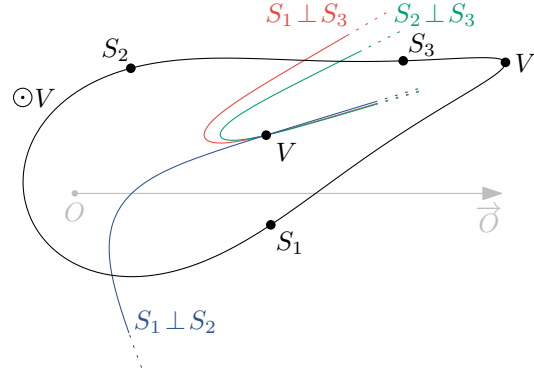
It remains to prove that changing the length of the line segment also changes the angle accordingly. Note that  $|\overline{AC}| < |\overline{AC'}|$  implies  $\cosh(|\overline{AC}|) < \cosh(|\overline{AC'}|)$ , since  $\cosh(x)$  is strictly increasing for increasing  $x \geq 0$ . Again, using the hyperbolic law of cosines, we can express  $\varphi$  using the lengths of the line segments in  $\triangle ABC$  as

$$\begin{aligned} \varphi &= \arccos\left(\frac{\cosh(|\overline{AB}|) \cosh(|\overline{BC}|) - \cosh(|\overline{AC}|)}{\sinh(|\overline{AB}|) \sinh(|\overline{BC}|)}\right) \\ &= \arccos\left(\frac{\cosh(|\overline{AB}|) \cosh(|\overline{BC'}|) - \cosh(|\overline{AC}|)}{\sinh(|\overline{AB}|) \sinh(|\overline{BC'}|)}\right) \\ &< \arccos\left(\frac{\cosh(|\overline{AB}|) \cosh(|\overline{BC'}|) - \cosh(|\overline{AC'}|)}{\sinh(|\overline{AB}|) \sinh(|\overline{BC'}|)}\right) \\ &= \varphi', \end{aligned}$$

where the inequality is due to the fact that  $\cosh(|\overline{AC}|) < \cosh(|\overline{AC'}|)$  and that  $\arccos(x)$  is strictly decreasing for increasing  $x$ . ◀

We note that in a degenerate triangle where the angle at  $B$  is  $\pi$ , the length of the segment opposite of  $B$  is given by the sum of the lengths of the other two segments. Thus, the above lemma confirms the fact that the triangle inequality also holds in the hyperbolic plane.

The following lemma shows that, if two points  $B, C$  have certain distances to a third point  $A$ , then every distance between the two distances is realized by a point on  $\overline{BC}$ .



■ **Figure 2** A point  $V$  with three sites  $S_1, S_2$ , and  $S_3$  on the arc of its witness circle  $\odot V$ . The far point  $V'$  is the point on  $\odot V$  with the largest distance to the pole  $O$ . The perpendicular bisectors of the sites intersect at  $V$ .

► **Lemma 2.** Let  $\triangle ABC$  be a triangle with  $|\overline{AB}| \leq |\overline{AC}|$ . For every  $d \in [|\overline{AB}|, |\overline{AC}|]$ , there exists a point  $P \in \overline{BC}$  with  $|\overline{AP}| = d$ .

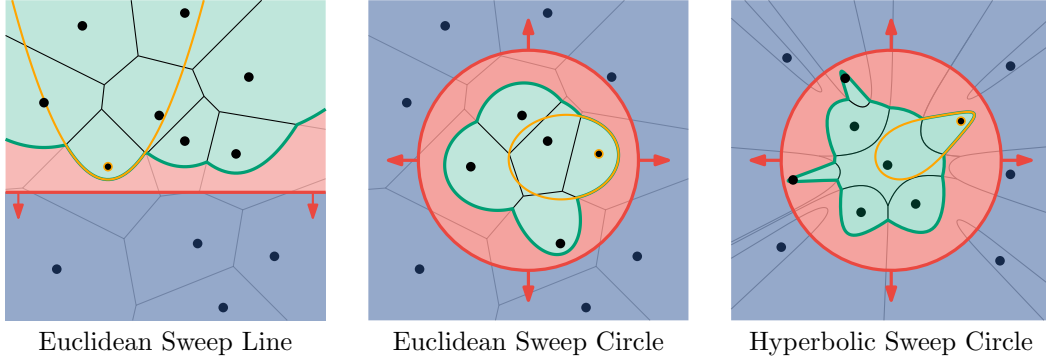
**Proof.** For  $d = |\overline{AB}|$  or  $d = |\overline{AC}|$ , the points  $P = B$  and  $P = C$  fulfill the requirements of the lemma, respectively. So assume that  $d \in (|\overline{AB}|, |\overline{AC}|)$ . Now consider the circle  $\odot A$  of radius  $d$  around  $A$ . Since  $|\overline{AB}| < d$ , the point  $B$  is inside the circle. Moreover, since  $|\overline{AC}| > d$ , the point  $C$  is outside the circle. Consequently, the line segment  $\overline{BC}$  intersects the circle at a point  $P = \overline{BC} \cap \odot A$ . In particular,  $P \in \odot A$  and thus  $|\overline{AP}| = d$ . ◀

## 2.1 Hyperbolic Voronoi Diagram

The hyperbolic Voronoi diagram is defined analogously to the Euclidean counterpart [10, Chapter 7]. Let  $\mathcal{S}$  be a set of finitely many points in  $\mathbb{H}^2$ , called *sites*. For each site  $S \in \mathcal{S}$  we define the *Voronoi cell*  $\text{Vor}(S)$  as the set of points  $P \in \mathbb{H}^2$  such that no site in  $\mathcal{S}$  is closer to  $P$  than  $S$ . The *Voronoi diagram*  $\text{Vor}(\mathcal{S})$  is the partition of  $\mathbb{H}^2$  into the Voronoi cells of the sites. The diagram is formalized by the set  $\mathcal{E}$  of *Voronoi edges* denoting the borders between cells, together with the set  $\mathcal{V}$  of *Voronoi vertices* denoting the endpoints of the edges. Note that, by definition, the Voronoi edge between two sites  $S_1 \neq S_2$  is a subset of the bisector  $S_1 \perp S_2$ . Further note that  $\mathcal{V}$  contains all points  $V \in \mathbb{H}^2$  that have three closest sites, i.e.,  $V \in \mathcal{V}$  if and only if it is the center of an empty circle  $\odot V$  with at least three sites  $S_1, S_2, S_3, \dots \in \mathcal{S}$  on its arc [6]. See Figure 2 for an illustration. We call this circle the *witness circle* of  $V$ . In the context of hyperbolic Voronoi diagrams, we are often interested in the point  $V' \in \odot V$ , denoted as the *far point* of  $V$ , that is farthest from the pole, i.e., the point with the largest radial coordinate among points on the witness circle of  $V$ . We call the sites  $S_1, S_2, S_3, \dots$  the *incident sites* of  $V$  and refer to the tuple containing the incident sites in the order one encounters them when traversing  $\odot V$  in clockwise direction starting at the far point  $V'$ , as the *incidence tuple* of  $V$ .

## 2.2 Fortune's Algorithm

**Euclidean Sweep Line.** Given a set  $\mathcal{S}$  of sites in the Euclidean plane, Fortune's algorithm [12] computes the Voronoi diagram  $\text{Vor}(\mathcal{S})$  using a *sweep line* that can be thought of as being parallel to the  $x$ -axis and traversing the plane in negative  $y$ -direction. See Figure 3 (left) for an illustration. At any time during the algorithm all sites above the sweep line are incorporated



■ **Figure 3** Illustration of Fortune’s algorithm and its adaptations. Black dots denote the sites. The sweep line (or circle) is dark red; arrows indicate its movement. The green region denotes the completed part of the diagram (black edges). The orange curve is the beach parabola (or ellipse) of the site with orange border. The beach line (or curve) is dark green. The red region denotes the part between sweep line (or circle) and beach line (or curve). Blue areas denote the unseen region.

into the diagram. The sites below the sweep line have not been seen, yet, and may affect the existing diagram, at least within a certain region above the sweep line. The boundary that separates this region from the part of the diagram that cannot be affected from sites below the sweep line is called the *beach line*. It consists of parts of *beach parabolas*, which contain the points that lie at equal distance between a site and the sweep line. The intersections of neighboring beach parabolas trace the edges of the Voronoi diagram. Maintaining the beach line is the crucial part of the algorithm. Of course, one cannot perform a continuous sweep motion in a computer program. Instead the algorithm makes use of the fact that the beach line only changes at certain sweep line positions, called *site events* and *circle events*. Site events occur when the sweep line reaches a site and a new beach parabola is added to the beach line. A circle event occurs when the sweep line reaches the lowest point of a circle containing three sites whose beach parabolas are consecutive on the beach line. There a parabola is potentially removed from the beach line and a Voronoi vertex is detected. For a more detailed description, we refer the reader to [10, Section 7.2].

**Euclidean Sweep Circle.** It was later shown that Fortune’s algorithm is actually a degenerate form of a *sweep circle* algorithm [28, Theorem 1]. Instead of a sweep line that traverses the plane, the idea is to use a *sweep circle* that grows from a certain point (see Figure 3 (center)). Then, beach parabolas become *beach ellipses* that contain the points at equal distance between a site and the sweep circle and the beach line becomes a *beach curve* consisting of beach ellipse segments. If one imagined the center of the sweep circle to lie at infinite distance to the sites, one obtains the original sweep line algorithm.

In this paper, we show that the sweep circle approach also works in the hyperbolic plane.

### 3 A Hyperbolic Sweep Circle Approach

In the polar-coordinate model, “straight” lines are hyperbolas that are bent towards the pole. Consequently, sweeping a line through the hyperbolic plane is rather tedious, as even the scheduling of site events leads to difficult computations. A much more natural approach is obtained by considering a sweep circle of expanding radius centered at the pole. This presents the first difference to the Euclidean approach: While the choice for the center of the

sweep circle is basically irrelevant in Euclidean space, the pole is the only reasonable choice in the hyperbolic plane, as the occurrence of site events can be easily read from the radii of the sites then. Scheduling circle events and handling events is more involved. As shown in Figure 3 (right), the hyperbolic counterparts of beach ellipses and the beach curve are rather different from their Euclidean versions. Nevertheless, the hyperbolic sweep circle approach works analogously to the Euclidean variant. The idea is to simulate the expansion of the sweep circle, whose increasing radius we denote with  $\hat{r}$ , and to maintain two data structures, which we describe in the following.

### 3.1 Beach Curve

In the Euclidean sweep line approach the beach line consists of parts of beach parabolas. For each site  $S \in \mathcal{S}$  above the sweep line, the beach parabola represents all points that lie at equal distance to  $S$  and the sweep line. In the generalized Euclidean sweep circle approach, these parabolas become beach ellipses. They are only defined for sites that are contained in the sweep circle, which we denote with  $\mathcal{S}_{\leq \hat{r}} = \{S \in \mathcal{S} \mid r(S) \leq \hat{r}\}$ , i.e., the set of sites whose radius is at most the radius of the sweep circle. The beach ellipse of a site  $S \in \mathcal{S}_{\leq \hat{r}}$  consists of all points that lie at equal distance to  $S$  and the sweep circle.

In the hyperbolic plane the beach ellipse of  $S$ , denoted by  $\mathcal{O}S$ , also contains all points that are equidistant from  $S$  and the sweep circle. However, the shape is not actually elliptic, as can be seen in Figure 3 (right). The following lemma shows how  $\mathcal{O}S$  can be parameterized by the angular coordinates of the points that lie on it. To this end, we define a function  $r_{\mathcal{O}S}(\varphi)$  that maps an angle  $\varphi \in [0, 2\pi)$  to the radius of the point  $P \in \mathcal{O}S$  with  $\varphi(P) = \varphi$ . See Figure 6 (right) for two exemplary functions.

► **Lemma 3.** *Let  $\hat{r} > 0$  be the radius of the sweep circle, let  $S \in \mathcal{S}_{\leq \hat{r}}$  be a site with  $r(S) < \hat{r}$ , and let  $P \in \mathbb{H}^2$  be a point with  $\varphi(P) = \varphi$ . Then,  $P \in \mathcal{O}S$  if and only if  $P$  has radius*

$$r_{\mathcal{O}S}(\varphi) = \operatorname{atanh} \left( \frac{\cosh(\hat{r}) - \cosh(r(S))}{\sinh(\hat{r}) - \sinh(r(S)) \cos(\varphi - \varphi(S))} \right).$$

**Proof.** By definition, we have  $P \in \mathcal{O}S$  if and only if  $P$  is equidistant to  $S$  and the sweep circle. Since the distance between a point and a circle centered at the origin is given by the difference of their radii,  $P$  needs to fulfill the equality

$$|\overline{PS}| = \hat{r} - r(P).$$

Applying Equation 2, which describes the hyperbolic distance between two points, together with an application of the hyperbolic cosine on both sides then yields

$$\cosh(r(P)) \cosh(r(S)) - \sinh(r(P)) \sinh(r(S)) \cos(\varphi(P) - \varphi(S)) = \cosh(\hat{r} - r(P)).$$

We can now apply the identity  $\cosh(x - y) = \cosh(x) \cosh(y) - \sinh(x) \sinh(y)$  to the right hand side and obtain

$$\begin{aligned} \cosh(r(P)) \cosh(r(S)) - \sinh(r(P)) \sinh(r(S)) \cos(\varphi(P) - \varphi(S)) = \\ \cosh(\hat{r}) \cosh(r(P)) - \sinh(\hat{r}) \sinh(r(P)). \end{aligned}$$

We continue by subtracting  $\cosh(\hat{r}) \cosh(r(P))$  on both sides and adding  $\sinh(\hat{r}) \sinh(r(P))$ , which yields

$$\begin{aligned} \sinh(\hat{r}) \sinh(r(P)) - \sinh(r(P)) \sinh(r(S)) \cos(\varphi(P) - \varphi(S)) = \\ \cosh(\hat{r}) \cosh(r(P)) - \cosh(r(P)) \cosh(r(S)). \end{aligned}$$



By factoring out  $\sinh(r(P))$  and  $\cosh(r(P))$ , we get

$$\sinh(r(P))(\sinh(\hat{r}) - \sinh(r(S)) \cos(\varphi(P) - \varphi(S))) = \cosh(r(P))(\cosh(\hat{r}) - \cosh(r(S))),$$

which is equivalent to

$$\frac{\sinh(r(P))}{\cosh(r(P))} = \frac{\cosh(\hat{r}) - \cosh(r(S))}{\sinh(\hat{r}) - \sinh(r(S)) \cos(\varphi(P) - \varphi(S))},$$

after dividing by  $\cosh(r(P))$  and  $\sinh(\hat{r}) - \sinh(r(S)) \cos(\Delta_\varphi(P, S))$  on both sides. Finally, we recognize that the left hand side is the hyperbolic tangent  $\tanh(r(P))$ . Applying the inverse hyperbolic tangent then yields the claim.  $\blacktriangleleft$

We note that, when the site  $S$  is not inside the sweep circle, but on its arc (i.e.,  $r(S) = \hat{r}$ ), then its beach ellipse degenerates into the line segment  $\mathcal{OS} = \overline{OS}$ .

The beach curve  $\mathcal{B}$  is defined as the set of points lying on the outer most parts of the beach ellipses, as shown in Figure 4 (left). More formally, we define the *active segments* of a site  $S \in \mathcal{S}_{\leq \hat{r}}$  as  $\mathcal{A}(\mathcal{OS}) = \{P \in \mathcal{OS} \mid \nexists S' \in \mathcal{S}_{\leq \hat{r}}, P' \in \mathcal{OS}' : \varphi(P) = \varphi(P') \wedge r(P) < r(P')\}$ . For an angular coordinate  $\varphi \in [0, 2\pi)$ , we say that a site  $S$  is *active at*  $\varphi$ , if there exists a point  $P \in \mathcal{A}(\mathcal{OS})$  with  $\varphi(P) = \varphi$ . The beach curve  $\mathcal{B}$  is then given by the union of the active segments of sites in the sweep circle, i.e.,  $\mathcal{B} = \bigcup_{S \in \mathcal{S}_{\leq \hat{r}}} \mathcal{A}(\mathcal{OS})$ .

Now consider two sites  $S, T \in \mathcal{S}_{\leq \hat{r}}$  together with an intersection  $P$  of their beach ellipses. The distance between  $P$  and the sweep circle is given by  $\hat{r} - r(P)$  and is, by definition of the beach ellipse, equal to  $|\overline{PS}|$  and to  $|\overline{PT}|$ . We obtain the following observation.

► **Observation 4.** *Let  $S, T \in \mathcal{S}_{\leq \hat{r}}$  be two sites with beach ellipses  $\mathcal{OS}$  and  $\mathcal{OT}$ , and let  $P \in \mathcal{OS} \cap \mathcal{OT}$  be a point on an intersection of them. Then,  $P$  lies on the perpendicular bisector  $S \perp T$ .*

Consequently, intersections of active beach ellipse segments move along the bisectors of the sites as the sweep circle expands, allowing us to trace the Voronoi edges, which are subsets of these bisectors (see Section 2.1).

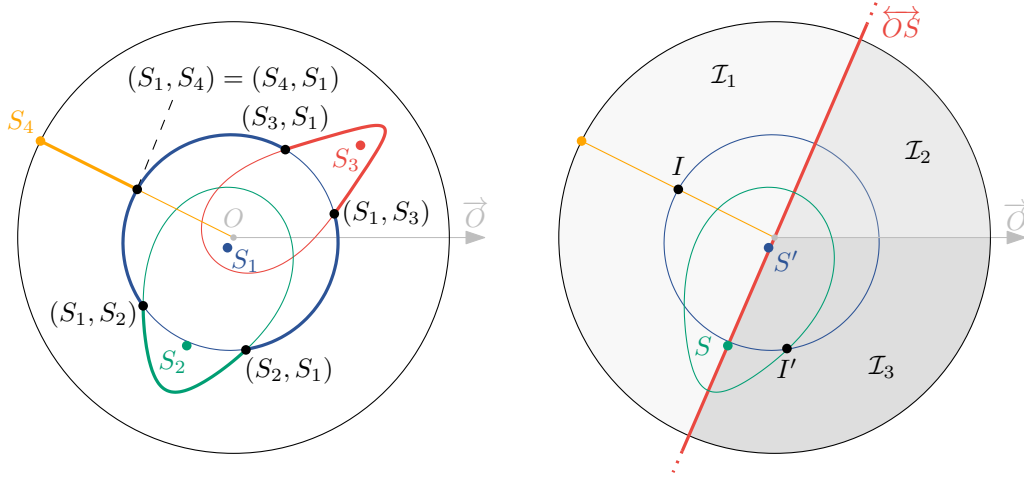
We represent the beach curve  $\mathcal{B}$  as a tuple  $\mathcal{I}$  of intersections of active beach ellipse segments that are ordered by their angular coordinates. Since the beach curve is circular, the beginning and end of this tuple are identified. Note that the angular coordinates of the intersections are constantly changing as the sweep circle expands. Therefore, we represent the intersections implicitly as a tuple of the two intersecting sites. More precisely, consider an active segment of a site  $S$ , that is bounded by the intersections  $I$  and  $I'$  with two other active segments belonging to the sites  $T$  and  $T'$ , respectively. If  $I$  and  $I'$  appear in this order when traversing the beach curve in counterclockwise direction, then the segment is represented by the corresponding tuples  $(T, S)$  and  $(S, T')$  in this order. See Figure 4 (left) for an illustration of intersection tuples.

As the sweep circle expands, intersections enter and leave the beach curve and the data structure  $\mathcal{I}$  needs to be maintained accordingly, while not knowing the angular coordinates of the intersections. For efficient insertions and deletions in  $\mathcal{I}$ , we propose the following procedure that allows us to perform a binary search, while potentially reducing the number of intersections whose actual coordinates need to be computed.

Consider a new intersection  $I$  that enters the beach curve and assume that its angular coordinate  $\varphi(I)$  is given<sup>1</sup>. In order to find its position in the data structure  $\mathcal{I}$  we want to

<sup>1</sup> As established in Section 4.1, this assumption is valid.





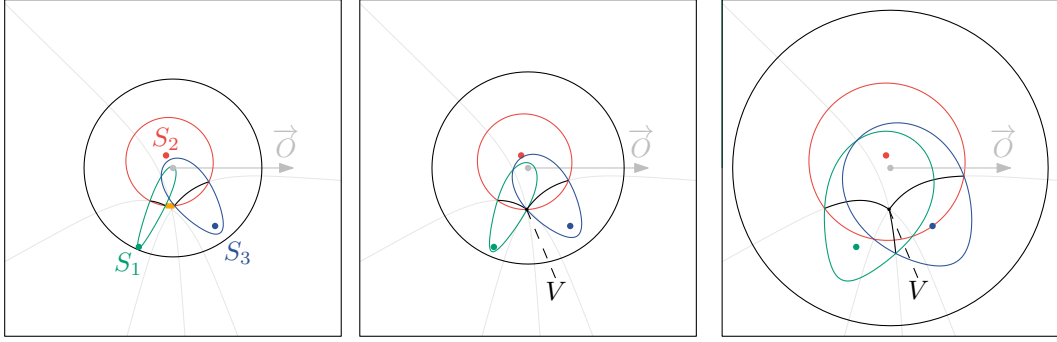
■ **Figure 4 (Left)** Four sites and their beach ellipses. Since  $S_4$  (orange) lies on the sweep circle (black), its beach ellipse is degenerate. Active segments are bold. Intersections are denoted as black points. **(Right)** When performing a binary search for a new intersection  $I$ , we implicitly compare its angle with the one of  $I'$  using the gray sectors  $\mathcal{I}_1, \mathcal{I}_2$ , and  $\mathcal{I}_3$  that are defined using the line  $\overleftrightarrow{OS'}$ .

perform a binary search and thus need to be able to decide whether  $\varphi(I) < \varphi(I')$  for a given intersection  $I' \in \mathcal{I}$ , where  $\varphi(I')$  is not known. Let  $S, S' \in \mathcal{S}_{\leq \hat{r}}$  be the two sites with  $I' \in \mathcal{OS} \cap \mathcal{OS}'$  and assume without loss of generality that  $r(S) \geq r(S')$ . The idea now is to use the line  $\overleftrightarrow{OS}$  to decide whether  $\varphi(I) < \varphi(I')$ . If  $\mathcal{OS}$  is degenerate, then  $\varphi(I') = \varphi(S)$  and the decision is straightforward. Otherwise, we split the angular interval  $[0, 2\pi)$  into three parts. Interval  $\mathcal{I}_1$  contains the angles of all points lying on the opposite side of  $\overleftrightarrow{OS}$  as the polar axis  $\vec{O}$ . Intervals  $\mathcal{I}_2$  and  $\mathcal{I}_3$  contain the angles on the same side of  $\overleftrightarrow{OS}$  as  $\vec{O}$  that are smaller and larger than  $\varphi(S)$ , respectively. See Figure 4 (right) for an illustration of the intervals. Then, if  $\varphi(I)$  and  $\varphi(I')$  are in different intervals, it is easy to decide whether  $\varphi(I) < \varphi(I')$ . Only if they are in the same interval do we need to compute the angular coordinate of  $I'$ . Thus, it may suffice to determine the intervals that  $\varphi(I)$  and  $\varphi(I')$  lie in, without computing  $\varphi(I')$  explicitly. Since  $\varphi(I)$  is given, determining its interval is trivial. Finding the one containing  $\varphi(I')$  is more involved. We can compute this information once when  $I'$  enters the beach curve, since we know its angular coordinate at this moment. Then, if  $I' \in \mathcal{I}_2$ , this does not change as the sweep circle expands (as a consequence of Lemma 9 below). However, if  $I' \in \mathcal{I}_1$  or  $I' \in \mathcal{I}_3$ , it may move from one interval to another by passing angular coordinate 0 as the sweep circle expands. Then  $I'$  moves from the first position in the beach curve data structure  $\mathcal{I}$  to the last or vice versa, which we call a *structure event*. Such events are scheduled or canceled every time the first or last element in  $\mathcal{I}$  changes.

In conclusion, we now know how to maintain  $\mathcal{I}$  and that we can use the contained intersections to trace the Voronoi edges. It remains to determine the events at which intersections enter and leave  $\mathcal{I}$  and how we can use them to detect the Voronoi vertices.

### 3.2 Event Queue

The second data structure that the algorithm maintains is a priority queue called *event queue*  $\mathcal{Q}$ , which stores the events at which the beach curve changes, in the order in which an expanding sweep circle encounters them. Each event is associated with a point in the plane and the priority of the event is equal to the radius of the point. Analogous to the Euclidean



■ **Figure 5** Beach curve intersections within an expanding sweep circle (black). **(Left)** An active segment (orange) of  $S_2$  (red) is about to vanish. **(Center)** The active segment has vanished as the intersections of  $\mathcal{OS}_1$  and  $\mathcal{OS}_3$  with  $\mathcal{OS}_2$  meet at a point  $V$ . **(Right)** The vanished segment is replaced by a single intersection of  $\mathcal{OS}_1$  and  $\mathcal{OS}_3$ .

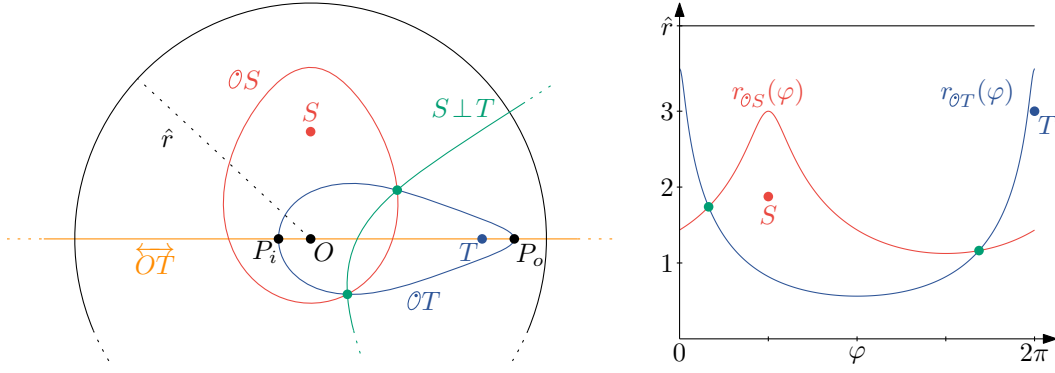
version (see Section 2.2), there are two types of events that change the beach curve by either adding or removing active beach ellipse segments.

An active beach ellipse segment is added to the beach curve when the sweep circle expands beyond a previously unseen site, i.e., when the radius  $\hat{r}$  of the sweep circle is equal to the radial coordinate of that site. (See site  $S_4$  in Figure 4 (left) for an example). When encountering such a *site event*, the intersections of the newly added active segment with an existing active segment are added to the tuple  $\mathcal{I}$  and the bisectors between the new site and the corresponding existing site are marked as part of the Voronoi diagram. Clearly, all site events can be scheduled in advance, since the radial coordinates of the sites are given.

On the other hand, an active beach ellipse segment can be removed from the beach curve, which happens when its two intersections with other active segments merge, as shown in Figure 5. Let  $S_1, S_2, S_3 \in \mathcal{S}_{\leq \hat{r}}$  be three sites such that an active segment of  $\mathcal{OS}_2$  intersects an active segment of  $\mathcal{OS}_1$  and one of  $\mathcal{OS}_3$ . When the two intersections merge at a point  $V$ , then  $V$  has equal distance to the sweep circle, as well as to the three sites  $S_1, S_2$ , and  $S_3$ . Consequently, all of them are incident to a circle  $\odot V$  that is completely contained in the sweep circle. Such an event is, therefore, called *circle event*. Note that no unseen site can lie in  $\odot V$ . Thus, if no site is contained in  $\odot V$  as the circle event occurs, then  $V$  is the center of an empty circle and, therefore, a Voronoi vertex (see Section 2.1). Then,  $V$  is added to the diagram and the bisectors of the incident sites are marked as being incident to  $V$ . Moreover, the tuple of active beach ellipse intersections  $\mathcal{I}$  is adjusted, by removing the merged intersections and replacing them with a new intersection of the corresponding active segments of  $\mathcal{OS}_1$  and  $\mathcal{OS}_3$ .

Such a circle event occurs when the sweep circle reaches the far point  $V'$  of  $V$ , i.e., the point with the largest radial coordinate among all points on  $\odot V$ . Thus, whenever an active segment enters or leaves the beach curve, we can use its intersections in  $\mathcal{I}$  to determine the neighboring active segments and schedule circle events by determining the point  $V'$  for the circle the corresponding sites are incident to. We note that not all tuples of consecutive beach curve intersections lead to a circle event, as the corresponding bisectors may not intersect or, even if they do, the beach ellipse intersections may diverge as the sweep circle expands. Consequently, we distinguish between *true* and *false* circle events. We refer to Lemma 12 for an explanation on how to decide whether a circle event is true or false.

Instead of a continuous sweep motion, the algorithm then computes the Voronoi diagram by iteratively processing the events in the event queue, until the queue is empty.



■ **Figure 6 (Left)** Two sites  $S, T$  inside the sweep circle (black). The points  $P_i$  and  $P_o$  are on  $\mathcal{O}T$  (blue) and are inside and outside of  $\mathcal{O}S$  (red), respectively. The intersections (green points) of the ellipses are on the perpendicular bisector  $S \perp T$  (green) and on opposite sites of the line  $\overrightarrow{OT}$  (orange). **(Right)** The functions  $r_{\mathcal{O}S}(\varphi)$  and  $r_{\mathcal{O}T}(\varphi)$  describe the arcs of the beach ellipses on the left.

## 4 Correctness and Complexity

In this section, we present the components for the proof of the following main theorem.

► **Theorem 5.** *Let  $\mathcal{S} = \{S_1, \dots, S_n\} \subset \mathbb{H}^2$  be a set of sites. Then, the sweep circle algorithm computes  $\text{Vor}(\mathcal{S})$  in time  $\mathcal{O}(n \log(n))$ .*

Like the algorithm itself, the proof of its correctness works analogous to the Euclidean version [10, Section 7.2]. Therefore, we only focus on the main parts of the proof and show that they also hold for the hyperbolic sweep circle approach. In particular, we show that the only way in which a new beach ellipse segment can appear on the beach curve is through a site event (Lemma 15), the only way in which an existing segment can disappear from the beach curve is through a circle event (Lemma 17), and that every Voronoi vertex is detected by means of a circle event (Lemma 18).

### 4.1 Beach Ellipse Intersections

To start, we establish some basic properties of beach ellipse intersections in the hyperbolic plane, beginning with their existence. Given a site  $S \in \mathcal{S}_{\leq \hat{r}}$ , we say that a point  $P$  is *inside* the beach ellipses  $\mathcal{O}S$ , if  $|\overline{PS}|$  is smaller than the distance between  $P$  and the sweep circle. If  $|\overline{PS}|$  is larger instead, we say that  $P$  is *outside* of  $\mathcal{O}S$ . The following lemma shows that, given two distinct sites inside the sweep circle, the beach ellipse of one contains two points that are inside and outside of the ellipse of the other, respectively, as illustrated in Figure 6 (left).

► **Lemma 6.** *Let  $\hat{r}$  be the radius of the sweep circle, let  $S \neq T \in \mathcal{S}_{\leq \hat{r}}$  be two sites with  $0 < r(S) \leq r(T) < \hat{r}$  and let  $\mathcal{O}S$  and  $\mathcal{O}T$  be their beach ellipses. Then the point  $P_i \in \mathcal{O}T$  with  $\varphi(P_i) = \varphi(T) + \pi$  is inside of  $\mathcal{O}S$  and  $P_o \in \mathcal{O}T$  with  $\varphi(P_o) = \varphi(T)$  is outside of  $\mathcal{O}S$ .*

**Proof.** Assume, without loss of generality, that  $\varphi(T) = 0$ . To show that  $P_i$  is inside of  $\mathcal{O}S$ , we show that the distance between  $P_i$  and the sweep circle is larger than  $|\overline{P_i S}|$ . More precisely, since  $P_i \in \mathcal{O}T$ ,  $P_i$  is equidistant to the sweep circle and to  $T$ . Consequently, it suffices to show that  $|\overline{P_i T}| > |\overline{P_i S}|$ . We now distinguish several cases depending on the position of  $S$ . If  $\varphi(S) = \varphi(T)$ , then we have  $r(S) < r(T)$  (since  $S \neq T$ ) and thus

$$|\overline{P_i T}| = r(P_i) + r(T) > r(P_i) + r(S) = |\overline{P_i S}|.$$

If  $\varphi(S) = \varphi(T) + \pi$ , we first consider the case where  $r(S) \geq r(P_i)$ . Then,

$$|\overline{P_i T}| = r(P_i) + r(T) \geq r(P_i) + r(S) > r(S) - r(P_i) = |\overline{P_i S}|.$$

Alternatively, if  $\varphi(S) = \varphi(T) + \pi$  and  $r(S) < r(P_i)$ , we have

$$|\overline{P_i T}| = |\overline{P_i S}| + r(S) + r(T) > |\overline{P_i S}|.$$

In all other cases, we can consider the triangle  $\triangle OSP_i$ . Since the area of this triangle is non-zero, we can apply the strict triangle inequality, which yields  $|\overline{P_i S}| < r(P_i) + r(S)$ . It follows that

$$|\overline{P_i T}| = r(P_i) + r(T) \geq r(P_i) + r(S) > |\overline{P_i S}|.$$

Consequently, in all cases  $P_i$  is closer to  $S$  than to the sweep circle, and is therefore inside  $\mathcal{O}S$ . Proving that  $P_o$  is outside of  $\mathcal{O}S$  works analogously. We show that  $P_o$  is closer to the sweep circle than to  $S$ , which is equivalent to showing  $|\overline{P_o T}| < |\overline{P_o S}|$ , since  $P_o$  is equidistant to  $T$  and the sweep circle. We again distinguish several cases depending on the position of  $S$ . If  $\varphi(S) = \varphi(T)$ , the distinctness of  $S$  and  $T$  implies  $r(S) < r(T)$  and thus

$$|\overline{P_o T}| = r(P_o) - r(T) < r(P_o) - r(S) = |\overline{P_o S}|.$$

Similarly, if  $\varphi(S) = \varphi(T) + \pi$ , we have

$$|\overline{P_o T}| = r(P_o) - r(T) < r(P_o) + r(S) = |\overline{P_o S}|.$$

Again, in all other cases, we can apply the strict triangle inequality to conclude  $r(P_o) < r(S) + |\overline{P_o S}|$  or equivalently  $r(P_o) - r(S) < |\overline{P_o S}|$ . Thus,

$$|\overline{P_o T}| = r(P_o) - r(T) \leq r(P_o) - r(S) < |\overline{P_o S}|,$$

which shows that  $P_o$  is outside of  $\mathcal{O}S$  in all cases. ◀

With the above lemma we can now prove that two non-degenerate beach ellipses intersect in exactly two points. If one of them is degenerate, they intersect in exactly one point.

► **Lemma 7.** *Let  $\hat{r}$  be the radius of the sweep circle, let  $S \neq T \in \mathcal{S}_{\leq \hat{r}}$  be two sites with  $0 < r(S) \leq r(T)$  and let  $\mathcal{O}S$  and  $\mathcal{O}T$  be their beach ellipses. Then,  $\mathcal{O}S \cap \mathcal{O}T$  contains two points if  $r(S), r(T) < \hat{r}$  and one point, otherwise.*

**Proof.** We start with the non-degenerate case and first show that the number of intersections is at least two, followed by a proof that it is at most two. By Lemma 3, the beach ellipse of  $S$  can be described by a function  $r_{\mathcal{O}S}(\varphi)$  that maps an angle  $\varphi \in [0, 2\pi)$  to the radius of the point  $P \in \mathcal{O}S$  with  $\varphi(P) = \varphi$ . Analogously, there is a function  $r_{\mathcal{O}T}(\varphi)$  for  $\mathcal{O}T$ . See Figure 6 (right) for an illustration. As shown in Lemma 6, there are two points  $P_i, P_o \in \mathcal{O}T$  that are inside and outside of  $\mathcal{O}S$ , respectively. Thus,  $r_{\mathcal{O}S}(\varphi(P_i)) > r_{\mathcal{O}T}(\varphi(P_i))$  and  $r_{\mathcal{O}S}(\varphi(P_o)) < r_{\mathcal{O}T}(\varphi(P_o))$ . Since  $r_{\mathcal{O}S}(\varphi), r_{\mathcal{O}T}(\varphi)$  are continuous and periodic functions with a period of  $2\pi$  (see Lemma 3), we can apply the intermediate value theorem to conclude that there are at least two values  $\varphi \in [0, 2\pi)$  such that  $r_{\mathcal{O}S}(\varphi) = r_{\mathcal{O}T}(\varphi)$ .

We continue by proving that the number of intersections is at most two. The angular coordinates of all intersections are obtained by solving  $r_{\mathcal{O}S}(\varphi) = r_{\mathcal{O}T}(\varphi)$  for  $\varphi$ . By Lemma 3, this is the case when

$$\frac{\cosh(\hat{r}) - \cosh(r(S))}{\sinh(\hat{r}) - \sinh(r(S)) \cos(\varphi - \varphi(S))} = \frac{\cosh(\hat{r}) - \cosh(r(T))}{\sinh(\hat{r}) - \sinh(r(T)) \cos(\varphi - \varphi(T))}.$$

Note that solving this equation for  $\varphi$  is equivalent to finding the roots of the function

$$f(\varphi) = a \cos(\varphi - \varphi(S)) - b \cos(\varphi - \varphi(T)) + c,$$

where the constants  $a, b$ , and  $c$  are defined as

$$\begin{aligned} a &= (\cosh(\hat{r}) - \cosh(r(T))) \sinh(r(S)), \\ b &= (\cosh(\hat{r}) - \cosh(r(S))) \sinh(r(T)), \text{ and} \\ c &= (\cosh(r(T)) - \cosh(r(S))) \sinh(\hat{r}). \end{aligned}$$

Further note that  $f(\varphi)$  is the sum of two differently phased cosine functions of equal frequency with amplitudes  $a$  and  $b$ , respectively, together with a constant  $c$ . Since the sum of two sinusoids of the same frequency is another sinusoid of that frequency, we can use [18, Equation (6)], to conclude that

$$f(\varphi) = a' \cos(\varphi + \xi) + c,$$

where the constants  $a'$  and  $\xi$  are given by

$$\begin{aligned} a' &= \sqrt{(a \cos(\varphi(S)) + b \cos(\varphi(T)))^2 + (a \sin(\varphi(S)) + b \sin(\varphi(T)))^2}, \\ \xi &= \text{atan} \left( \frac{a \sin(\varphi(S)) + b \sin(\varphi(T))}{a \cos(\varphi(S)) + b \cos(\varphi(T))} \right), \end{aligned}$$

and  $a, b$ , and  $c$  are defined as above. Consequently,  $f(\varphi)$  is a cosine function with amplitude  $a'$  and period  $2\pi$ , which has at most two roots in  $[0, 2\pi)$  if  $a' \neq 0$ . Therefore, it remains to show that  $a'$  is non-zero. First note that  $a'$  only vanishes if both sums in the quadratic functions do. Since there exists no  $x \in \mathbb{R}$  such that  $\cos(x) = 0$  and  $\sin(x) = 0$ , it follows that  $a'$  is non-zero as long as  $a$  and  $b$  are non-zero. Since  $\mathcal{O}S$  and  $\mathcal{O}T$  are non-degenerate, we know that  $r(S), r(T) < \hat{r}$ , and since  $\cosh(x)$  is strictly increasing for  $x \geq 0$ , we have

$$\cosh(\hat{r}) - \cosh(r(S)) > 0 \text{ and } \cosh(\hat{r}) - \cosh(r(T)) > 0.$$

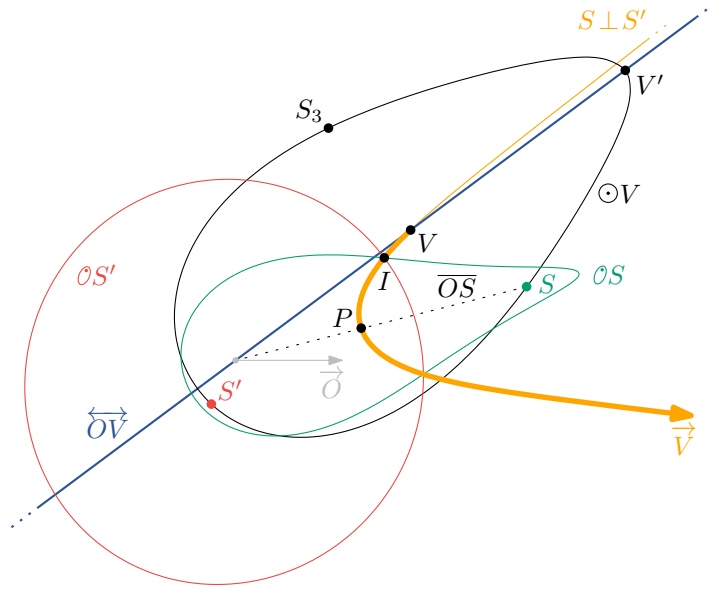
Moreover, since  $r(S), r(T) > 0$  by assumption, it follows that  $\sinh(r(S)), \sinh(r(T)) > 0$ , which concludes the proof of the non-degenerate case.

If  $\mathcal{O}S$  is degenerate, then  $\mathcal{O}S = \overline{OS}$ . It follows that all intersections in  $\mathcal{O}S \cap \mathcal{O}T$  have angular coordinate  $\varphi(S)$ , and by Lemma 3, there is only one point  $P \in \mathcal{O}T$  satisfying  $\varphi(P) = \varphi(S)$ . Analogously, there is only one intersection when  $\mathcal{O}T$  is degenerate but  $\mathcal{O}S$  is not. Finally, when both sites are degenerate, i.e.,  $r(S) = r(T) = \hat{r}$ , then  $\varphi(S) \neq \varphi(T)$ , since both sites are assumed to be distinct. In that case, the two ellipses  $\mathcal{O}S = \overline{OS}$  and  $\mathcal{O}T = \overline{OT}$  intersect only in the pole. ◀

We continue by investigating how the intersections move as the sweep circle expands. To this end, we first show that the beach ellipses expand as well.

► **Lemma 8.** *Let  $S \in \mathcal{S}_{\leq \hat{r}}$  be a site and let  $r_1, r_2$  be two radii with  $r(S) \leq r_1 < r_2$ . Then,  $\mathcal{O}S$  at  $\hat{r} = r_1$  is inside of  $\mathcal{O}S$  at  $\hat{r} = r_2$ .*

**Proof.** Consider a point  $P \in \mathcal{O}S$  as  $\hat{r} = r_1$ . Then, the distance between  $P$  and the sweep circle is given by  $r_1 - r(P)$  and is equal to  $|\overline{PS}|$ . At  $\hat{r} = r_2$ ,  $|\overline{PS}|$  remains unchanged. However, then the distance between  $P$  and the sweep circle increases to  $r_2 - r(P) > r_1 - r(P) = |\overline{PS}|$ . It follows that  $P$  is closer to  $S$  than to the sweep circle at  $\hat{r} = r_2$  and is therefore inside  $\mathcal{O}S$ . ◀



■ **Figure 7** Illustration of the proof of Lemma 10. The sites  $S$  and  $S'$  lie on the witness circle of  $V$ . The intersection  $I \in \mathcal{OS} \cap \mathcal{OS}'$  that moves towards  $V$  lies on the angular bisector  $\overrightarrow{V}$  (orange) of the angle  $\angle SVS'$ , since  $\overrightarrow{V}$ ,  $I$ ,  $P$ , and  $S$  are on the same side of  $\overleftrightarrow{OV}$ .

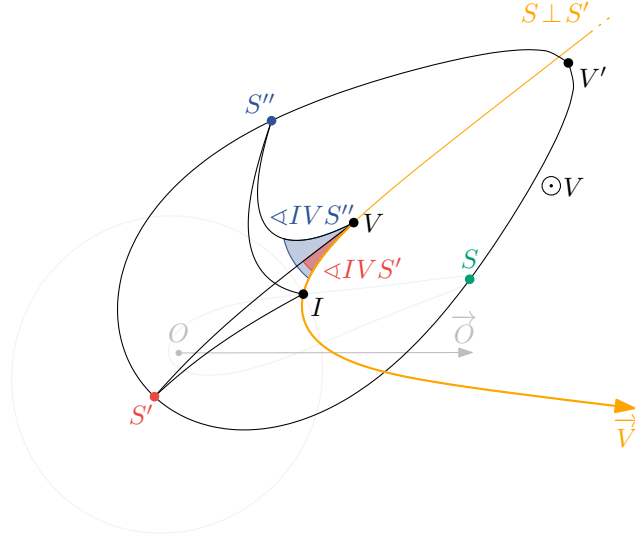
We are now ready to show that the two beach ellipse intersections of a pair of sites  $S$  and  $T$  start at the same point and move along the bisector  $S \perp T$  in opposite directions as the radius  $\hat{r}$  of the sweep circle increases.

► **Lemma 9.** *Let  $S \neq T \in \mathcal{S}_{\leq \hat{r}}$  be two sites with  $r(S) \leq r(T)$  and consider the intersections  $I, I' \in \mathcal{OS} \cap \mathcal{OT}$  and the point  $P = \overline{OT} \cap S \perp T$ . For  $\hat{r} = r(T)$ , we have  $I = I' = P$ . For  $\hat{r} > r(T)$ ,  $I$  and  $I'$  are on opposite sides of  $\overleftrightarrow{OT}$ . As  $\hat{r}$  increases, so do  $|PI|$  and  $|PI'|$ .*

**Proof.** For  $\hat{r} = r(T)$ , the beach ellipse  $\mathcal{O}T$  is degenerate and consists of the line segment  $\overline{OT}$ . By Lemma 7, the two ellipses  $\mathcal{O}S$  and  $\mathcal{O}T$  intersect in a single point. This point is  $P$  as the intersection is on  $\mathcal{O}T = \overline{OT}$  and has by definition equal distance to  $S$  and  $T$ , i.e., it lies on  $S \perp T$ . Moreover, this point is unique, as  $\overline{OT} \not\subset S \perp T$ , since  $T \in \overline{OT}$  but  $T \notin S \perp T$ .

We continue with the proof that  $I$  and  $I'$  are on opposite sides of  $\overleftrightarrow{OT}$  for  $\hat{r} > r(T)$ , as shown in Figure 6 (left). Without loss of generality, assume that  $\varphi(T) = 0$  and consider the points  $P_i, P_o \in \mathcal{OT}$  as defined in Lemma 6, that are inside and outside of  $\mathcal{OS}$ , respectively. That is,  $r_{\mathcal{OT}}(0) > r_{\mathcal{OS}}(0)$  and  $r_{\mathcal{OT}}(\pi) < r_{\mathcal{OS}}(\pi)$ . Consequently, one of  $I$  and  $I'$  has an angular coordinate in  $(0, \pi)$  and the other in  $(\pi, 2\pi)$ . Thus, they are on opposite sides of  $\overleftrightarrow{OT}$ .

It remains to show that  $|\overline{PI}|$  and  $|\overline{PI'}|$  increase with  $\hat{r}$ . Consider two radii  $r_1, r_2$  with  $r(T) \leq r_1 < r_2$ . Let  $I_{r_1}$  and  $I_{r_2}$  denote the positions that the intersection  $I$  has at  $\hat{r} = r_1$  and  $\hat{r} = r_2$ , respectively, and let  $I'_{r_1}$  and  $I'_{r_2}$  be defined analogously. Consider  $\hat{r} = r_1$  first. By Lemma 7 the bisector  $S \perp T$  intersects  $\mathcal{OT}$  at exactly the points  $I_{r_1}$  and  $I'_{r_1}$ , meaning the line segment  $\overline{I_{r_1}I'_{r_1}}$  lies in  $\mathcal{OT}$ . Moreover, the point  $P$  lies in  $\mathcal{OT}$  and on  $S \perp T$ , meaning  $P \in \overline{I_{r_1}I'_{r_1}}$  and thus the line segments  $\overline{PI_{r_1}}$  and  $\overline{PI'_{r_1}}$  are contained in  $\mathcal{OT}$ . Now assume that  $\hat{r}$  increases to  $\hat{r} = r_2$  but  $|\overline{PI}|$  does not. (The proof for  $|\overline{PI'}|$  is analogous.) Then  $I_{r_2} \in \overline{PI_{r_1}}$ . However, since the beach ellipse  $\mathcal{OT}$  at  $\hat{r} = r_1$  is completely contained in  $\mathcal{OT}$  at  $\hat{r} = r_2$  (Lemma 8), it follows that  $I_{r_2} \in \overline{PI_{r_1}}$  is inside of  $\mathcal{OT}$ , contradicting the fact that  $I_{r_2} \in \mathcal{OT}$ .  $\blacktriangleleft$



■ **Figure 8** Illustration of the proof of Corollary 11. Since  $\angle IVS' < \angle IVS''$  the distance from  $I$  to  $S'$  is smaller than the one to  $S''$ .

The above lemma has some interesting implications. Consider two sites  $S, T$  that are incident to a Voronoi vertex  $V$ , meaning they lie on the arc of the witness circle of  $V$ . Then,  $V$  lies on the bisector  $S \perp T$  and, in particular, on one side of the point  $P \in S \perp T$  defined in the lemma. As the sweep circle expands, the intersections  $I$  and  $I'$  move along the bisector and away from  $P$ , meaning exactly one of them reaches  $V$  eventually. More precisely, the following lemma captures from which directions the intersections approach a Voronoi vertex. Recall that  $\angle ABC$  denotes the angle between  $\overrightarrow{BA}$  and  $\overrightarrow{BC}$  in clockwise direction around  $B$ .

► **Lemma 10.** *Let  $V \in \mathcal{V}$  be a Voronoi vertex with far point  $V'$  and incidence tuple  $(S_1, S_2, S_3)$ . Further, let  $(S, S') \in \{(S_1, S_2), (S_2, S_3), (S_1, S_3)\}$ , let  $\vec{V}$  be the angular bisector of  $\angle SVS'$ , and let  $I \in \partial S \cap \partial S'$  be the intersection with  $I = V$  at  $\hat{r} = r(V')$ . Then,  $I \in \vec{V}$  for  $\hat{r} < r(V')$ .*

**Proof.** Note that  $V$  divides  $S \perp S'$  into the two rays  $\vec{V}$  and  $S \perp S' \setminus \vec{V}$  and so does the line  $\overleftrightarrow{OV}$ . Thus, since  $I \in S \perp S'$ , it suffices to show that  $I$  and  $\vec{V}$  are on the same side of  $\overleftrightarrow{OV}$ . Without loss of generality, assume  $r(S) \geq r(S')$ . By Lemma 9 there is a point  $P = \overline{OS} \cap S \perp S'$  such that  $I \in \overline{PV} \subset S \perp S'$ . Thus,  $P$  and  $I$  are on the same side of  $\overleftrightarrow{OV}$ . Moreover, since  $P \in \overline{OS}$ , we also know that  $S$  and  $I$  are on the same side of  $\overleftrightarrow{OV}$ . Consequently, it suffices to show that  $\vec{V}$  is on the same side of  $\overleftrightarrow{OV}$  as  $S$ , as shown in Figure 7.

If  $S'$  is on the same side of  $\overleftrightarrow{OV}$  as  $S$ , then this is trivially true, since  $\vec{V}$  is the angular bisector of  $\angle SVS'$ . Thus, let  $S$  and  $S'$  lie on opposite sides of  $\overleftrightarrow{OV}$  and consider the angles  $\varphi_S = \angle SVO$  and  $\varphi_{S'} = \angle OVS'$ . Since  $\vec{V}$  is the angle bisector of  $\angle SVS'$ , we know that the angle between  $\overrightarrow{VS}$  and  $\vec{V}$  is  $1/2(\varphi_S + \varphi_{S'})$ . To show that  $\vec{V}$  is on the same side of  $\overleftrightarrow{OV}$  as  $S$ , it then suffices to show that  $1/2(\varphi_S + \varphi_{S'}) \leq \varphi_S$  or equivalently that  $\varphi_{S'} \leq \varphi_S$ . To this end, we make use of the hyperbolic law of cosines.

Consider the triangles  $\triangle OVS$  and  $\triangle OVS'$  and note that  $\varphi_S$  and  $\varphi_{S'}$  are the angles at  $V$ , respectively. Moreover, since  $S$  and  $S'$  lie on the witness circle of  $V$ , we have  $|\overline{VS}| = |\overline{VS'}|$ . If  $r(S') = r(S)$ , the side lengths of the triangles match and we have  $\varphi_S = \varphi_{S'}$  by Equation (1). If  $r(S') < r(S)$ , i.e., if  $|\overline{OS'}| < |\overline{OS}|$ , we can apply Lemma 1 to conclude that  $\varphi_{S'} < \varphi_S$ . ◀



As a corollary of the above lemma, we can conclude that before the sweep circle radius reaches the far point  $V'$  of  $V$ , there are two intersections whose distance to the sites of the intersecting beach ellipses is smaller than two the third site.

► **Corollary 11.** *Let  $V \in \mathcal{V}$  be a Voronoi vertex with far point  $V'$  and incidence tuple  $(S_1, S_2, S_3)$ . Further, let  $(S, S', S'') \in \{(S_1, S_2, S_3), (S_2, S_3, S_1)\}$  and consider the intersection  $I \in \mathcal{OS} \cap \mathcal{OS}'$  with  $I = V$  at  $\hat{r} = r(V')$ . Then,  $|\overrightarrow{IS''}| > |\overrightarrow{IS}| = |\overrightarrow{IS'}|$  for  $\hat{r} < r(V')$ .*

**Proof.** Without loss of generality, assume that  $\angle S'VS'' \leq \angle S''VS$ . Consider the two triangles  $\triangle IVS'$  and  $\triangle IVS''$ , as illustrated in Figure 8, and note that  $|\overrightarrow{VS'}| = |\overrightarrow{VS''}|$ , since  $S'$  and  $S''$  lie on the witness circle of  $V$ . By Lemma 10, we know that  $I$  lies on the angle bisector  $\overrightarrow{V}$  of  $\angle SVS'$ , meaning  $I$  lies between  $\overrightarrow{VS}$  and  $\overrightarrow{VS'}$  in clockwise direction around  $V$ . By definition of the incidence tuple, we know that  $S''$  does not lie between  $\overrightarrow{VS}$  and  $\overrightarrow{VS'}$  in clockwise direction, meaning  $\angle IVS' < \angle IVS''$ . Consequently, we can apply Lemma 1 to conclude that  $|\overrightarrow{IS}| = |\overrightarrow{IS'}| < |\overrightarrow{IS''}|$ . ◀

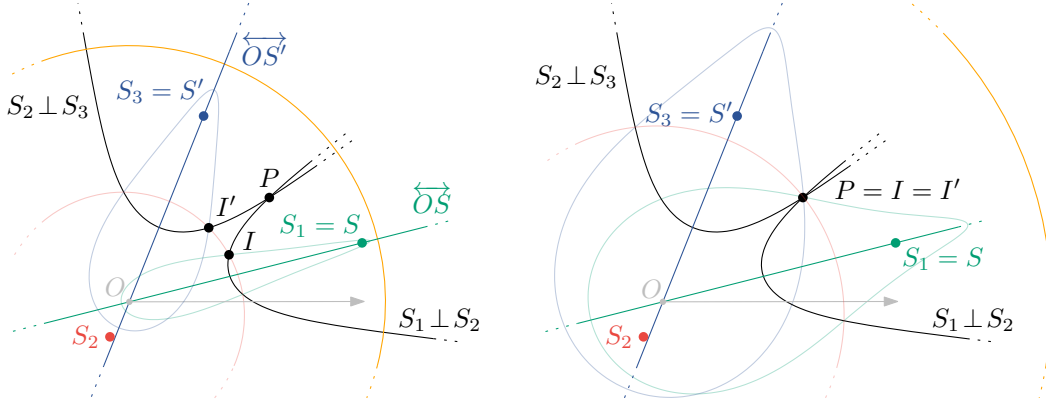
Finally, we investigate how we can use the beach ellipse intersections to predict circle events and how to distinguish between true and false ones (see Section 3.2). Predicting the event is straightforward, as we only need to compute the intersection  $P$  of the two bisectors corresponding to two beach ellipse intersections that are consecutive<sup>2</sup> on the beach curve. We note that  $P$  may not exist, in which case no circle event is predicted. If it does exist, we need to determine whether the two beach ellipse intersections converge towards  $P$  as the sweep circle expands. To this end, let  $S_1$  and  $S_2$  be two sites and recall that an intersection  $I \in \mathcal{OS}_1 \cap \mathcal{OS}_2$  moves away from the line through the pole and the site with the larger radius (Lemma 9). We call this site the *dominant site* of  $I$ . The following lemma now says that, as the sweep circle expands, two beach ellipse intersections meet at a point  $P$  (predicting a true circle event), if  $P$  and the intersections are on the same side of the lines through the pole and the dominant sites. See Figure 9 for an illustration.

► **Lemma 12.** *Let  $S_1, S_2, S_3 \in \mathcal{S}_{\leq \hat{r}}$  be distinct and let  $P \in \mathbb{H}^2$  lie at distance  $d$  to them. Further, let  $r < r(P) + d$  be such that  $I \in \mathcal{OS}_1 \cap \mathcal{OS}_2$  and  $I' \in \mathcal{OS}_2 \cap \mathcal{OS}_3$  are distinct at  $\hat{r} = r$  and let  $S$  and  $S'$  be their dominant sites, respectively. Then,  $P = I = I'$  at  $\hat{r} = r(P) + d$ , if and only if  $P$  and  $I$  (resp.  $I'$ ) are on the same side of  $\overleftrightarrow{OS}$  (resp.  $\overleftrightarrow{OS'}$ ) at  $\hat{r} = r$ .*

**Proof.** We give the proof for  $I$  and  $\overleftrightarrow{OS}$ . The one for  $I'$  and  $\overleftrightarrow{OS'}$  is analogous. Note that the positions of the sites and thus the coordinates of  $S$  and  $P$  are fixed. Consequently,  $P$  is on the same side of  $\overleftrightarrow{OS}$  at all times. Moreover, by Lemma 9 the intersection  $I$  is on the same side of  $\overleftrightarrow{OS}$  at all times. It follows that, if and only if  $P$  and  $I$  are on the same side of  $\overleftrightarrow{OS}$  at a given sweep circle radius, then this holds for all sweep circle radii.

When  $\hat{r} = r(P) + d$ , the sweep circle has equal distance to  $P$  as to all sites  $S_1, S_2$ , and  $S_3$ , meaning  $P$  lies on their beach ellipses. In particular, we have  $P = I$ . Clearly,  $P$  and  $I$  lie on the same side of  $\overleftrightarrow{OS}$  at that point. By the above argumentation, then and only then does the same hold at  $\hat{r} = r$ . ◀

<sup>2</sup> We argue in the proof of Lemma 18 that it suffices to consider consecutive intersections.



■ **Figure 9** Illustration of the proof of Lemma 12. **(Left)** The sweep circle (orange) has radius  $\hat{r} < r(P) + d$ . The point  $P$  and the intersections  $I$  and  $I'$  are on the same sides of  $\vec{OS}$  and  $\vec{OS'}$ , respectively. **(Right)** The intersections meet at  $P$  when  $\hat{r} = r(P) + d$ .

## 4.2 Active Beach Ellipse Segments

In this section, we consider how the beach curve changes as the sweep circle expands. We start by proving the following lemma, which characterizes when beach ellipse intersections are active, i.e., when they are on the beach curve  $\mathcal{B}$ , as depicted in Figure 10.

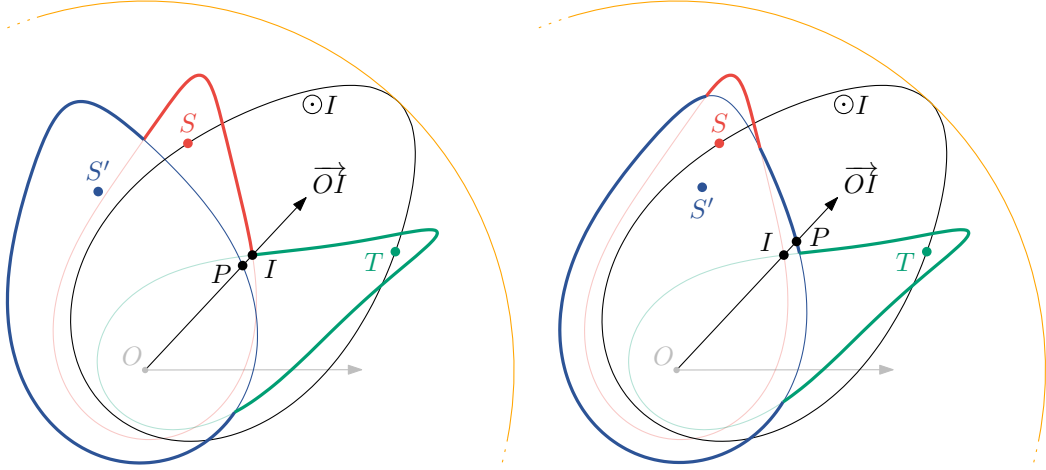
► **Lemma 13.** *Let  $S, T \in \mathcal{S}_{\leq \hat{r}}$  be two sites and let  $I \in \mathcal{OS} \cap \mathcal{OT}$  be an intersection of their ellipses. Then,  $I \in \mathcal{B}$  if and only if there exists no site  $S' \in \mathcal{S}_{\leq \hat{r}}$  with  $S' \neq S, T$  such that  $|\overrightarrow{S'I}| < |\overrightarrow{SI}| = |\overrightarrow{TI}|$ .*

**Proof.** We start by proving that  $S'$  does not exist if  $I \in \mathcal{B}$ . To this end, we show for each  $S' \in \mathcal{S}_{\leq \hat{r}}$  with  $S' \neq S, T$ , that  $|\overrightarrow{S'I}| \geq |\overrightarrow{SI}| = |\overrightarrow{TI}|$ . Consider the intersection  $P \in \overrightarrow{OI} \cap \mathcal{OS'}$ . Since  $I \in \mathcal{B}$ , we know that  $r(I) \geq r(P)$ , meaning  $I$  is not inside the beach ellipse  $\mathcal{OS'}$ . Thus,  $I$  is at least as close to the sweep circle as to  $S'$ . Since the distance between  $I$  and the sweep circle is given by  $\hat{r} - r(I)$ , it follows that  $|\overrightarrow{S'I}| \geq \hat{r} - r(I) = |\overrightarrow{SI}| = |\overrightarrow{TI}|$ .

It remains to consider the case where  $I \notin \mathcal{B}$ . Then, there exists a beach ellipse segment of another site  $S' \neq S, T$  that is active at angular coordinate  $\varphi(I)$ . That is, there is a point  $P = \overrightarrow{OI} \cap \mathcal{OS'}$  such that  $r(I) < r(P)$ . It follows that  $I$  is inside of  $\mathcal{OS'}$ , meaning  $I$  is closer to  $S'$  than to the sweep circle. We can conclude that  $|\overrightarrow{S'I}| < \hat{r} - r(I) = |\overrightarrow{SI}| = |\overrightarrow{TI}|$ . ◀

With the above lemma, we are now ready to investigate how changes to the beach curve are related to the events in the queue  $\mathcal{Q}$ . Consider the tuple  $\bar{\mathcal{Q}}$ , that contains all site events and all true circle events (see Section 3.2). Recall that  $V'$  denotes the far point of a Voronoi vertex  $V \in \mathcal{V}$ , i.e., the point with the maximum radial coordinate among points on the witness circle of  $V$ . Then,  $\bar{\mathcal{Q}} = (r_0, r_1, \dots, r_k, r_{k+1})$  contains the radii  $r_0 = 0$ ,  $r_{k+1} = \infty$  and all radii  $\{r(S) \mid S \in \mathcal{S}\} \cup \{r(V') \mid V \in \mathcal{V}\}$  in ascending order inbetween. We note that  $\bar{\mathcal{Q}}$  is different from  $\mathcal{Q}$ , since the latter also contains structure events and may contain scheduled circle events that are later canceled, e.g., when a site is detected within the corresponding witness circle.

For two sites  $S, T \in \mathcal{S}_{\leq \hat{r}}$ , we say that a point  $P \in \mathcal{OS} \cap \mathcal{OT}$  enters the beach curve at radius  $r$ , if there is an  $\varepsilon > 0$  such that  $P \notin \mathcal{B}$  for  $\hat{r} \in [r - \varepsilon, r)$  and  $P \in \mathcal{B}$  when  $\hat{r} = r$ . Analogously, we say that  $P \in \mathcal{OS} \cap \mathcal{OT}$  leaves the beach curve at radius  $r$  if  $P \in \mathcal{B}$  when  $\hat{r} = r$  and there is an  $\varepsilon > 0$  such that  $P \notin \mathcal{B}$  for  $\hat{r} \in (r, r + \varepsilon]$ . In the following, we show that no beach ellipse intersection enters or leaves the beach curve between two events in  $\bar{\mathcal{Q}}$ .



■ **Figure 10** Illustration of the proof of Lemma 13. The circle  $\odot I$  contains all points that lie at equal distance to  $I$  as  $S$  and  $T$ . Note that this circle is tangent to the sweep circle (orange). **(Left)** The intersection  $I$  is on the beach curve (bold), since  $S$  and  $T$  are closer to  $I$  than  $S'$ . **(Right)** The intersection  $I$  is not on the beach curve, since  $S'$  is closer to  $I$  than  $S$  and  $T$ .

► **Lemma 14.** Let  $\bar{\mathcal{Q}}$  be the tuple of site events and true circle events and let  $r_i, r_j \in \bar{\mathcal{Q}}$  be two consecutive events. Then, for all  $\hat{r} \in (r_i, r_j)$  no beach ellipse intersection enters the beach curve.

**Proof.** Let  $S, T$  be two sites and let  $I \in \mathcal{OS} \cap \mathcal{OT}$  be an intersection of their ellipses. For the sake of contradiction, assume that there exists an  $r \in (r_i, r_j)$  such that  $I$  enters the beach curve at  $r$ . Note that no site event occurs in  $(r_i, r_j)$ , since this would contradict the construction of  $\bar{\mathcal{Q}}$ . Consequently, if  $I$  is on the beach curve at  $\hat{r} = r$ , we know that  $I$  is contained in the sweep circle for all  $\hat{r} \in (r_i, r_j)$ . By Lemma 13 we know that  $I$  not being on the beach curve before  $\hat{r} = r$  implies the existence of at least one site  $S' \neq S, T$ , such that  $|\overline{S'I}| < |\overline{SI}| = |\overline{TI}|$ . In particular, we choose  $S'$  to be the one that remains active the longest at angular coordinate  $\varphi(I)$  as the sweep circle expands beyond  $r_i$ . Since  $I$  is on the beach curve at  $\hat{r} = r$ , we also know that  $|\overline{S'I}| \geq |\overline{SI}| = |\overline{TI}|$  at that moment (again Lemma 13). Thus, as  $I$  moves along the bisector  $S \perp T$ , there exists an  $r' \in (r_i, r]$  such that  $|\overline{S'I}| = |\overline{SI}| = |\overline{TI}|$  (Lemma 2). Then,  $I$  is the center of an empty circle (as otherwise there would be yet another site that is longer active than  $S'$ , contradicting the choice of  $S'$ ) and thus lies on a Voronoi vertex  $V \in \mathcal{V}$ . However, this would imply that  $r' \in (r_i, r_j)$  is the radius of the far point of  $V$ , which again contradicts the construction of  $\bar{\mathcal{Q}}$ . ◀

Note that if no intersections enter the beach curve between events in  $\bar{\mathcal{Q}}$ , then also no beach ellipse segments can become active then. Moreover, no segments become active during a circle event either, as only two intersections are merged into one there. We can conclude the following lemma, which is the hyperbolic sweep circle counterpart of [10, Lemma 7.6] in the Euclidean sweep line version.

► **Lemma 15.** The only way in which a new beach ellipse segment can become active is through a site event.

We continue by investigating how beach ellipse segments disappear from the beach curve. Analogous to the proof of Lemma 14, we can prove that no beach ellipse intersection leaves the beach curve between two events in  $\bar{\mathcal{Q}}$ .

► **Lemma 16.** *Let  $\bar{Q}$  be the tuple of site events and true circle events and let  $r_i, r_j \in \bar{Q}$  be two consecutive events. Then, for all  $\hat{r} \in (r_i, r_j)$  no beach ellipse intersection leaves the beach curve.*

**Proof.** Consider two sites  $S, T$ , let  $I \in \mathcal{OS} \cap \mathcal{OT}$  be an intersection of their ellipses, and assume for the sake of contradiction that there exists an  $r \in (r_i, r_j)$  such that  $I$  leaves the beach curve at  $r$ . That is, there exists an  $\varepsilon > 0$ , such that  $I$  is on the beach curve until  $\hat{r} = r$  and is no longer on the beach curve for  $\hat{r} \in (r, r + \varepsilon)$ . By Lemma 13, it follows that for all sites  $S' \neq S, T$  we have  $|\overline{S'I}| \geq |\overline{SI}| = |\overline{TI}|$  at  $\hat{r} = r$ , but at least one of them is closer to  $I$  than  $|\overline{SI}| = |\overline{TI}|$  afterwards. Let  $S''$  be the one for which this happens first. That is, for this site we have  $|\overline{S''I}| \geq |\overline{SI}| = |\overline{TI}|$  at  $\hat{r} = r$  and  $|\overline{S''I}| < |\overline{SI}| = |\overline{ST}|$  afterwards. By Lemma 2, we know that when  $I$  moves along the bisector  $S \perp T$  as the sweep circle expands, there exists a radius  $r' \in [r, r + \varepsilon)$  such that  $|\overline{S''I}| = |\overline{SI}| = |\overline{TI}|$  when  $\hat{r} = r'$ . As by the choice of  $S''$ , no other site is closer to  $I$  than  $S'', S$ , and  $T$ , we know that  $I$  is the center of an empty circle and thus lies on a Voronoi vertex  $V \in \mathcal{V}$ . However, this implies that  $r' \in (r_i, r_j)$  is the radius of the far point of  $V$ , which contradicts the construction of  $\bar{Q}$ . ◀

Again, note that if no intersections can leave the beach curve between events in  $\bar{Q}$ , then also no beach ellipse segment can become inactive then. Moreover, no segments become inactive during a site event, since we only insert two intersections consecutively on the beach curve there. As a result, we obtain the following lemma, which is the hyperbolic equivalent of [10, Lemma 7.7] in the Euclidean sweep line approach.

► **Lemma 17.** *The only way in which an active beach ellipse segment can become inactive is through a circle event.*

### 4.3 Voronoi Vertices

It remains to prove that all Voronoi vertices are actually found by means of circle events. To simplify this proof, we make the assumption that at most three sites are incident to a Voronoi vertex  $V \in \mathcal{V}$ , meaning no more than three sites lie on its witness circle. If this assumption does not hold, the algorithm may produce duplicate Voronoi vertices, which need to be merged in a post-processing step. The following lemma is the analog of [10, Lemma 7.8] in the Euclidean version.

► **Lemma 18.** *Every Voronoi vertex is detected by means of a circle event.*

**Proof.** Let  $V \in \mathcal{V}$  be a Voronoi vertex, let  $V'$  be its far point, and let  $(S_1, S_2, S_3)$  be the incidence tuple of  $V$ . Further, let  $r \in \bar{Q}$  be the predecessor of  $r(V')$  in  $\bar{Q}$ . To show that  $V$  is detected by means of a circle event, we prove that for all sweep circle radii  $\hat{r} \in [r, r(V'))$  there are beach ellipse intersections  $I_{12} \in \mathcal{OS}_1 \cap \mathcal{OS}_2$  and  $I_{23} \in \mathcal{OS}_2 \cap \mathcal{OS}_3$  that are consecutive on the beach curve  $\mathcal{B}$ . Then, it follows that the corresponding circle event is in the event queue  $\mathcal{Q}$  and the Voronoi vertex is detected at  $\hat{r} = r(V')$ .

We start by showing that  $I_{12}, I_{23} \in \mathcal{B}$  for  $\hat{r} \in [r, r(V'))$ . In particular, we give the proof for  $I_{12}$ , as the one for  $I_{23}$  is analogous. For the sake of contradiction, assume that there exists an  $r' \in [r, r(V'))$  such that  $I_{12} \notin \mathcal{B}$  when  $\hat{r} = r'$ . By Lemma 7,  $I_{12}$  exists, so the only way for it *not* to be on the beach curve is that there exists another site  $S \neq S_1, S_2$  such that  $|\overline{SI_{12}}| < |\overline{S_1I_{12}}| = |\overline{S_2I_{12}}|$  (Lemma 13). Moreover, by Corollary 11 we have  $|\overline{S_3I_{12}}| > |\overline{S_1I_{12}}| = |\overline{S_2I_{12}}|$ . It follows that  $S \neq S_3$ . We now show that the site  $S$  that is distinct from  $S_1, S_2$ , and  $S_3$  cannot exist.

By Lemma 14 we know that  $I_{12}$  does not enter the beach curve until at least  $\hat{r} = r(V')$ . Now first consider the case where  $I_{12}$  enters the beach curve exactly at  $\hat{r} = r(V')$ , i.e., exactly when  $I_{12} = V$ . This means that  $|\overline{SI_{12}}| \geq |\overline{S_1I_{12}}| = |\overline{S_2I_{12}}|$  at this point (Lemma 13). In particular, we have  $|\overline{SI_{12}}| = |\overline{S_1I_{12}}| = |\overline{S_2I_{12}}|$  then, as by Lemma 2 there exists a point at which we have equality but this point does not occur before  $\hat{r} = r(V')$ . It follows that besides  $S_1, S_2$ , and  $S_3$ , the site  $S$  is on the witness circle of  $V$ , contradicting our assumption that no more than three sites do. Now consider the case where  $I_{12}$  does not enter the beach curve at  $\hat{r} = r(V')$ , i.e., when  $I_{12} = V$ . By Lemma 13, we know that  $|\overline{SI_{12}}| < |\overline{S_1I_{12}}|$ , i.e.,  $|\overline{SV}| < |\overline{S_1V}|$ , which means that  $S$  is contained in the witness circle of  $V$ , contradicting the assumption that  $V$  is a Voronoi vertex. Since both cases lead to a contradiction, we can conclude that  $I_{12} \in \mathcal{B}$  for all  $\hat{r} \in [r, r(V'))$ .

It remains to show that  $I_{12}$  and  $I_{23}$  are also consecutive on  $\mathcal{B}$  for  $\hat{r} \in [r, r(V'))$ . First note that any intersection that were to lie between  $I_{12}$  and  $I_{23}$  cannot span beyond these two intersections, as this would contradict the fact that  $I_{12}, I_{23} \in \mathcal{B}$ , which we just proved. It follows that if  $I_{12}, I_{23}$  are not consecutive on  $\mathcal{B}$ , then there are at least two intersections  $I$  and  $I'$  between them that belong to the same active segment  $\mathcal{A}$ , which is part of the beach ellipse of another site  $S$ . Since none of the intersections  $I_{12}, I_{23}, I$ , and  $I'$  leave  $\mathcal{B}$  until at least  $\hat{r} = r(V')$  (Lemma 16), it follows that  $I$  and  $I'$  stay between  $I_{12}$  and  $I_{23}$  until  $\hat{r} = r(V')$ , which is when  $I_{12}$  and  $I_{23}$  meet at  $V$ . Then,  $V = I_{12} = I_{23} = I = I'$ . Now note that only three intersections of the beach ellipses of the sites  $S_1, S_2$ , and  $S_3$  meet at  $V$ , since the two beach ellipse intersections of a pair of them travel in opposite directions on the perpendicular bisector, only one of which leads to  $V$  (Lemma 9). Thus, at least one of  $I$  and  $I'$  belongs to a beach ellipse  $\mathcal{OS}$  with  $S \neq S_1, S_2, S_3$ . It follows that a fourth site lies on the witness circle of  $V$ , contradicting the assumption that no more than three do.  $\blacktriangleleft$

#### 4.4 Complexity

To conclude the proof of Theorem 5, it remains to show that the algorithm takes time  $\mathcal{O}(n \log(n))$  to compute the Voronoi diagram of  $n$  sites. Initially, all site events need to be scheduled, meaning the sites have to be sorted by their radii, which takes time  $\mathcal{O}(n \log(n))$ . The running time of the remainder of the algorithm then depends on the complexity of the diagram, i.e., the number of Voronoi vertices and edges. It was previously shown that this complexity is  $\mathcal{O}(n)$ , by examining different models: the Poincaré disk model [6, Consequence of Proposition 2], the Poincaré half-plane model [9, Theorem 18.5.1] and the Klein disk model [21, Theorem 1]. Of course, it is no surprise that all came to the same conclusion, since the different models represent different ways to address points in the same space.

Clearly, there are exactly  $n$  site events and the number of true circle events is bounded by the number of Voronoi vertices, which is  $\mathcal{O}(n)$ . As each event is processed, at most a constant number of circle events are scheduled and as the algorithm proceeds the number of canceled events cannot be larger. Moreover, since each intersection can contribute at most one structure event, it follows that the total number of processed events is  $\mathcal{O}(n)$ .

It remains to show that we can handle an event in time  $\mathcal{O}(\log(n))$ . Since the queue contains  $\mathcal{O}(n)$  events, inserting and removing elements from the queue, takes time  $\mathcal{O}(\log(n))$ . Regarding updating the beach curve data structure, recall that two beach ellipses intersect at most two times (Lemma 7) and note that, consequently, at most two intersections are on the same edge of the Voronoi diagram at all times. It follows that the number of elements in the beach curve is at most  $\mathcal{O}(n)$  at all times, meaning insertions and deletions take at most  $\mathcal{O}(\log(n))$  time. All other operations, like inserting vertices to the diagram, marking bisectors incident to the vertices, and predicting new circle and structure events, take constant time.

## 5 Outlook

We present the first algorithm for computing Voronoi diagrams natively in the polar-coordinate model of the two-dimensional hyperbolic plane. We note that the distance function in this model generalizes nicely to higher dimensions, as only the computation of the angular distance between two points changes (one has to compute the central angle). Consequently, we believe that the hyperbolic sweep circle approach can be extended to higher dimensions. Furthermore, it would be interesting to extend the method to allow for computations of higher-order Voronoi diagrams, as they are useful in the context of nearest-neighbor queries.

A more direct application of our algorithm is the efficient computation of the hyperbolic counterpart to Euclidean minimum spanning trees. To the best of our knowledge *hyperbolic random minimum spanning trees* have not been studied before, but may prove useful as the tree equivalent to the aforementioned hyperbolic random graph model [16]. Analogous to the Euclidean version, the hyperbolic minimum spanning tree is a subgraph of the hyperbolic Delaunay complex of a given set of sites, meaning it can be computed in time  $\mathcal{O}(n \log(n))$  using our approach. Consequently, it would be interesting to implement our hyperbolic sweep circle method in order to generate and investigate trees in the hyperbolic plane.

---

## References

- 1 Gregorio Alanis-Lobato, Pablo Mier, and Miguel Andrade-Navarro. The latent geometry of the human protein interaction network. *Bioinformatics*, 34:2826–2834, 2018. doi:10.1093/bioinformatics/bty206.
- 2 Marshall Bern and David Eppstein. Optimal Möbius Transformations for Information Visualization and Meshing. In *Algorithms and Data Structures (WADS)*, pages 14–25, 2001. doi:10.1007/3-540-44634-6\_3.
- 3 Thomas Bläsius, Philipp Fischbeck, Tobias Friedrich, and Maximilian Katzmann. Solving vertex cover in polynomial time on hyperbolic random graphs. *Theory of Computing Systems*, 2021. doi:10.1007/s00224-021-10062-9.
- 4 Thomas Bläsius, Cedric Freiberger, Tobias Friedrich, Maximilian Katzmann, Felix Montenegro-Retana, and Marianne Thieffry. Efficient Shortest Paths in Scale-Free Networks with Underlying Hyperbolic Geometry. In *International Colloquium on Automata, Languages, and Programming (ICALP)*, pages 20:1–20:14, 2018. doi:10.4230/LIPIcs.ICALP.2018.20.
- 5 Martin Bock, Amit Kumar Tyagi, Jan-Ulrich Kreft, and Wolfgang Alt. Generalized Voronoi Tessellation as a Model of Two-dimensional Cell Tissue Dynamics. *Bulletin of Mathematical Biology*, 72(7):1696–1731, 2010. doi:10.1007/s11538-009-9498-3.
- 6 Mikhail Bogdanov, Olivier Devillers, and Monique Teillaud. Hyperbolic Delaunay complexes and Voronoi diagrams made practical. *Journal of Computational Geometry*, 5:56–85, 2014. doi:10.20382/JOCG.V5I1A4.
- 7 Marian Boguna, Fragiskos Papadopoulos, and Dmitri Krioukov. Sustaining the Internet with Hyperbolic Mapping. *Nature Communications*, 1(1):62, 2010. doi:10.1038/ncomms1063.
- 8 Jean-Daniel Boissonnat, André Cérézo, Olivier Devillers, and Monique Teillaud. Output-sensitive construction of the Delaunay triangulation of points lying in two planes. *International Journal of Computational Geometry and Applications*, 06(01):1–14, 1996. doi:10.1142/S0218195996000022.
- 9 Jean-Daniel Boissonnat and Mariette Yvinec. *Non-Euclidean metrics*. Cambridge University Press, 1998. doi:10.1017/CB09781139172998.025.
- 10 Mark de Berg, Otfried Cheong, Marc van Kreveld, and Mark Overmars. *Computational Geometry: Algorithms and Applications*. Springer, 2008.
- 11 David S. Ebert, F. Kenton Musgrave, Darwyn Peachey, Ken Perlin, and Steven Worley. *Texturing and Modeling: A Procedural Approach*. Elsevier Science, 2002.



- 12 Steven Fortune. A sweepline algorithm for Voronoi diagrams. In *Symposium on Computational Geometry (SoCG)*, page 313–322, 1986. doi:10.1145/10515.10549.
- 13 Guillermo García-Pérez, Marián Boguñá, Antoine Allard, and M. Serrano. The hidden hyperbolic geometry of international trade: World trade atlas 1870–2013. *Scientific Reports*, 6:33441, 2016. doi:10.1038/srep33441.
- 14 Santiago Garrido, Luis Moreno, Mohamed Abderrahim, and Fernando Martin. Path Planning for Mobile Robot Navigation using Voronoi Diagram and Fast Marching. In *2006 IEEE/RSJ International Conference on Intelligent Robots and Systems*, pages 2376–2381, 2006. doi:10.1109/IRoS.2006.282649.
- 15 Luca Gugelmann, Konstantinos Panagiotou, and Ueli Peter. Random hyperbolic graphs: Degree sequence and clustering. In *International Colloquium on Automata, Languages, and Programming (ICALP)*, page 573–585, 2012. doi:10.1007/978-3-642-31585-5\_51.
- 16 Dmitri Krioukov, Fragkiskos Papadopoulos, Maksim Kitsak, Amin Vahdat, and Marián Boguñá. Hyperbolic geometry of complex networks. *Physical Review E*, 82:036106, 2010. doi:10.1103/PhysRevE.82.036106.
- 17 Anton Krohmer. *Structures & algorithms in hyperbolic random graphs*. Dissertation, Universität Potsdam, 2016.
- 18 Richard G. Lyons. Sum of two sinusoids. 2011. URL: [https://dspguru.com/files/Sum\\_of\\_Two\\_Sinusoids.pdf](https://dspguru.com/files/Sum_of_Two_Sinusoids.pdf).
- 19 Tobias Müller and Merlijn Staps. The diameter of kpkvb random graphs. *Advances in Applied Probability*, 51(2):358–377, 2019. doi:10.1017/apr.2019.23.
- 20 Frank Nielsen. On Voronoi Diagrams on the Information-Geometric Cauchy Manifolds. *Entropy*, 22(7), 2020. doi:10.3390/e22070713.
- 21 Frank Nielsen and Richard Nock. Hyperbolic Voronoi Diagrams Made Easy. In *International Conference on Computational Science and Its Applications (ICCSA)*, page 74–80, 2010. doi:10.1109/ICCSA.2010.37.
- 22 Frank Nielsen and Richard Nock. Visualizing Hyperbolic Voronoi Diagrams. In *Proceedings of the Thirtieth Annual Symposium on Computational Geometry*, page 90–91, 2014. doi:10.1145/2582112.2595647.
- 23 Zahra Nilforoushan and Ali Mohades. Hyperbolic Voronoi Diagram. In *Computational Science and Its Applications (ICCSA)*, page 735–742, 2006. doi:10.1007/11751649\_81.
- 24 Kensuke Onishi and Nobuki Takayama. Construction of Voronoi Diagram on the Upper Half-Plane. *IEICE Transactions on Fundamentals of Electronics, Communications and Computer Sciences*, 79:533–539, 1996.
- 25 Arlan Ramsay and Robert D. Richtmyer. *Introduction to Hyperbolic Geometry*. Springer, 1995. doi:10.1007/978-1-4757-5585-5.
- 26 Michael Ian Shamos. *Computational Geometry*. Dissertation, Department of Computer Science, Yale University, 1977.
- 27 Toshihiro Tanuma, Hiroshi Imai, and Sonoko Moriyama. *Revisiting Hyperbolic Voronoi Diagrams in Two and Higher Dimensions from Theoretical, Applied and Generalized Viewpoints*, pages 1–30. Springer Berlin Heidelberg, 2011. doi:10.1007/978-3-642-25249-5\_1.
- 28 Shi-Qing Xin, Xiaoning Wang, Jiazhi Xia, Wolfgang Mueller-Wittig, Guo-Jin Wang, and Ying He. Parallel computing 2D Voronoi diagrams using untransformed sweepcircles. *Computer-Aided Design*, 45(2):483–493, 2013. doi:10.1016/j.cad.2012.10.031.